46th Annual Review of Progress in Quantitative Nondestructive Evaluation
QNDE2019
July 14-19, 2019, Portland, OR, USA

QNDE2019-1234

ARRAY BASED GUIDED WAVE MULTI-MODE DISPERSION CORRECTION

Andrew Downs[1], Ron Roberts[2],
Center for Nondestructive Evaluation
Ames, IA

ABSTRACT

This work seeks to implement a high frequency guided wave pulse-echo inspection which automatically isolates signals carried by multiple guided modes, then corrects for loss of temporal resolution arising from dispersive propagation. The measurement extracts wavenumber vs. frequency spectra through analysis of data collected with a phased array transducer designed for guided wave transduction. The goal is to provide a pulse-echo measurement that displays robust performance, similar to bulk wave measurements, without regard to the number of modes generated, or the frequency band of operation. This abstract summarizes the principles of the measurement and data analysis.

Keywords: guided wave, dispersion compensation,

NOMENCLATURE

ω	Radial frequency (rad/sec)
k	Spatial frequency (rad/m)
u_2	Normal particle displacement on plate
τ_{22}	Normal traction on plate

1. INTRODUCTION

Ultrasonic guided waves are multimodal and dispersive, making source or defect localization in plates and pipes difficult. To avoid this issue inspections are often performed using a narrowband pulse and specific types of transducers to excite single modes over frequency ranges in which $d\omega/dk$ of the dispersion curve is nearly constant. A signal processing technique first developed by Wilcox in [1], enables the effects of dispersion to be removed through application of temporal and spatial Fourier transforms. Roberts et al. in [2], extended the technique to multimodal dispersion compensation in an aluminum plate, using spatial array data obtained by mechanical scanning of contact transducers. Numerical results in [2] demonstrated the viability of the method. However, the robustness of the method was limited, by inconsistent coupling of scanned transducers to the surface of the plate. To overcome this limitation, a new measurement configuration is being explored using a novel phased array design. The measurement format and data processing in this approach are summarized here.

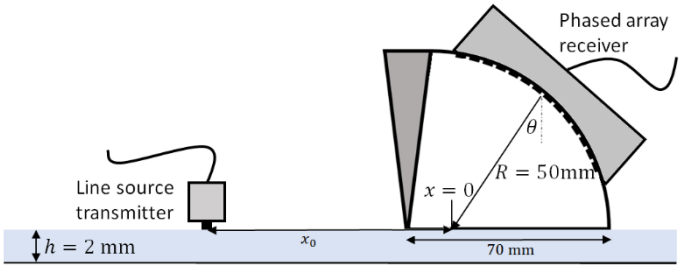

FIGURE 1: GUIDED WAVE ARRAY MEASUREMENT

2. MATERIALS AND METHODS

The underlying configuration of the measurement is depicted in Figure (1). To simplify discussion, a 2D conception of measurement is considered. A point source traction, normal to the surface, generates guided modes which propagate a distance x_0 to a receiver, which detects the normal particle displacements $\underline{u}_2(x,t)$ on the surface of the plate. The underscore indicates $\underline{u}_2(x,t)$ is a function of time. The propagating multimode signals are expressed in the frequency domain ω as a superposition of *N* mode contributions

$$u_2(x,\omega) = \sum_n^N \hat{u}_2^n(\omega) e^{ik_n(\omega)(x_o+x)} \quad (1)$$

where $k_n(\omega)$ is the frequency dependent wave number of the nth mode, known *a priori* for a plate of given thickness and material properties. The coordinate origin x=0 is taken as the focal point of the array transducer shown in Figure (1) on the plate surface. The goal of the measurement is to determine the source location

[1] Contact author: rroberts@iastate.edu
[2] Contact author: awdowns@iastate.edu

x_0 through analysis of the received guided wave signals. To facilitate discussion, Eq.(1) is re-written

$$u_2(x,\omega) = \sum_n^N \bar{u}_2^n(\omega) e^{ik_n(\omega)x} \quad (2)$$

$$\bar{u}_2^n(\omega) = \hat{u}_2^n(\omega) e^{ik_n(\omega)x_0} \quad (3)$$

where the dependence of $\bar{u}_2^n(\omega)$ on x_0 is implicitly assumed. It is noted that if $\underline{u}_2(x,t)$ were known for all time and space, the source location could be readily identified by observing the spatial support of $\underline{u}_2(x,t)$ at t=0. Equivalently, if $\bar{u}_2^n(\omega)$ were known for mode n, the location of the source could be determined by evaluating the inverse temporal Fourier transform

$$\underline{u}_2{}^n(x,0) = \frac{1}{2\pi}\int \bar{u}_2^n(\omega) e^{ik_n(\omega)x} d\omega$$

$$= \frac{1}{2\pi}\int \hat{u}_2^n(\omega) e^{ik_n(\omega)(x_0+x)} d\omega \quad (4)$$

It is evident in examining the second integral in Eq.(4) that the phase dispersion introduced by guided mode propagation is removed when $x = -x_0$. When the source has compact support, such as the applied point traction in Fig.(1), evaluation of eq.(4) will yield a spike located at $x=-x_0$. The goal of data measurement and processing is therefore the determination of the mode contributions $\bar{u}_2^n(\omega)$.

2.1 Extraction of Mode Contributions

The quantity measured in experiment is not the displacements $\underline{u}_2(x,t)$, but rather the response voltage $\underline{v}(t)$ of measurement system (transducer plus instrumentation) to the displacements. Application of Auld's reciprocity principle [3] to the measurement of Figure (1) is expressed

$$V(\omega) = \Gamma(\omega)\int \tau_{22}(x,\omega) u_2(x,\omega) dx \quad (5)$$

where $\tau_{22}(x,\omega)$ is the normal traction generated on the plate by the receiver when operated reciprocally as a transmitter, and $\Gamma(\omega)$ represents the transduction efficiency. Using Eqs.(2,3) in Eq.(5) yields

$$V(\omega) = \sum_n^N \bar{u}_2^n(\omega)\int \tau_{22}(x,\omega) e^{ik_n(\omega)x} dx \quad (6)$$

The integral in Eq. (6) is recognized at the spatial Fourier transform of the applied traction, denoted $\hat{\tau}_{22}(k,\omega)$, evaluated at spatial frequency $k=k_n(\omega)$. The voltage signal from the receiver is then expressed

$$V(\omega) = \Gamma(\omega)\sum_n^N \bar{u}_2^n(\omega)\hat{\tau}_{22}(k_n(\omega),\omega) \quad (7)$$

Note that were $\hat{\tau}_{22}(k,\omega)$ centered at $k_m(\omega)$ such that

$$\hat{\tau}_{22}(k_m(\omega) - k_n(\omega),\omega) = \delta nm \quad (8)$$

where δnm is the Kronecker delta, the m^{th} mode contribution would be determined simply as

$$\bar{u}_2^m(\omega) = \frac{V(\omega)}{\Gamma(\omega)} \quad (9)$$

Eq.(8) would hold were $\tau_{22}(x,\omega)$ to approach a plane wave displaying spatial frequency $k=k_n(\omega)$ on the plate surface. Since a plane wave is a physical impossibility, an approximation of a plane wave is sought in the physical measurement. To this end, the phased array depicted in Figure (1) was designed and procured, with which the desired property Eq.(8) is approximated as best as can through electronic phasing and/or post processing.

2.2 Implementation

The phased array is a 64-element, 2.25 MHz cylindrical array with a radius of 50 mm. 18 mm long (elevation) elements are centered over a Rexolite® wedge ($c_w = 2350$ m/s) at theta = 45° with an element pitch of 1mm. The array was fabricated for ISU by Imasonic.

While the array has a natural focus of 50 mm, the objective of the array is to generate beams with planar phase fronts with variable angles of incidence about a common footprint center at x=0 on the bottom surface of the wedge. To this end, groups of neighboring elements (e.g. 19) are phased so as to remove the natural phase front curvature from the resulting beam. Additionally, Hanning window apodization is added to the grouped aperture to reduce beam side lobe responses. The center of the element grouping is moved over the array surface electronically, to form 64 different receiving beam orientations. Apertures approaching the edges of the array are truncated by the finite array size. The spatial frequency spectra on the plate surface associated with each beam is roughly centered about

$$k_i = (\omega/c_w)\sin\theta_i \quad (10)$$

where c_w is the longitudinal wave velocity in the wedge, and θ_i is the angle at which the center element of the i^{th} beam is mounted on the array, as depicted in Figure(1). For the following discussion, the θ_i dependence is explicitly included in eq.(7)

$$V(\omega,\theta_i) = \Gamma(\omega)\sum_n^N \bar{u}_2^n(\omega)\hat{\tau}_{22}(k_n(\omega),\omega,\theta_i) \quad (11)$$

Assuming the received signals consist of N propagating modes, a system of NxN equations for $\bar{u}_2^n(\omega)$ can be generated at each frequency ω by selecting N angles in eq.(10) for which $(\omega/c_W)\sin(\theta_m)=k_m(\omega)$. However, it was deemed simpler and more robust to view Eq.(11) as an overdetermined system of 64 equations, and derived an NxN system by variational methods, leading to

$$\sum_n^N \bar{u}_2^n(\omega)\sum_{i=1}^{64}\hat{\tau}_{22}(k_n(\omega),\omega,\theta_i)\,\hat{\tau}_{22}^*(k_m(\omega),\omega,\theta_i) = \sum_{i=1}^{64} V(\omega,\theta_i)\,\hat{\tau}_{22}^*(k_m(\omega),\omega,\theta_i) \quad , m=1,..,N \quad (12)$$

where ()* denotes complex conjugation. After mode contributions $\bar{u}_2^n(\omega)$ are extracted, location of the source is determined using Eq. (4).

3. RESULTS AND DISCUSSION

Application of source location using the measurement configuration in Figure (1) is demonstrated using synthetic data. A model for plate wave generation by a point traction applied normal to the surface is used to compute displacements $u_2(x,t)$ on the surface beneath the wedge in Figure (1). The point source is positioned 7 cm from the receiver, and is assumed to display a temporal response described by a Hanning window with a

frequency spectrum centered at 2.25 MHz, and 100% bandwidth. The response of the array transducer was modeled assuming the piezoelectric array element imparts a traction normal to the wedge surface. The longitudinal and shear wave fields generated by the element are evaluated within the wedge, and the resulting normal traction transmitted out the bottom of the wedge into the coupling medium between the wedge and plate is computed. These normal tractions are computed for each of the 64 array elements. The normal traction generated by the various elements are then phased, weighted, and summed to generate 64 corresponding beams, as described above. Auld's reciprocity, as seen in Eq.(5), is used to compute the signal recorded from the array transducer for each of the 64 beams in response to guided wave field in the plate. The data received by the 64 beams is plotted as an image in Figure (2), and displays the modulus of spectral data as image brightness in the θ–ω plane. The beam angles vary from 9° to 81°. The accumulation of spectral energy along the dispersion curves for the plate is clearly evident. The dispersion curves for the plate plotted as θ–ω are explicitly overlaid on the v(ω,θ) data in the bottom image of Figure (2). At each frequency ω, the system of equations Eq.(12) is solved for the mode contributions $\bar{u}_2^n(\omega)$ using the data of Figure (2) as input to the right-hand-side of the equation. The mode contributions $\bar{u}_2^n(\omega)$ are then used in Eq.(4) to determine source location. The evaluation of Eq.(4) is plotted in Figure (3) for modes A0 and S0. A spike is clearly indicated at x=-7 cm, which is the location of the synthetic source.

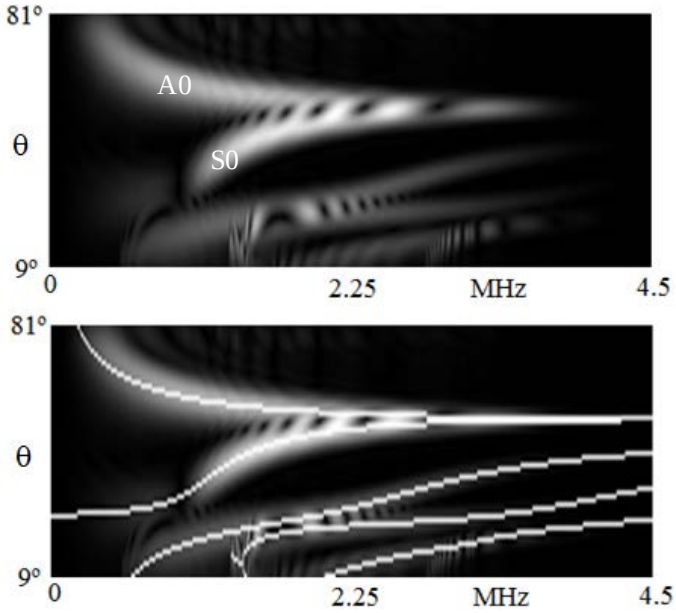

FIGURE 2: (TOP) SYNTHETIC $V(\omega,\theta)$ DATA (BOTTOM) DISPERSION CURVES OVERLAYING SYNTHETIC DATA.

4. CONCLUSION

A guided wave measurement was demonstrated in the preceding discussion that automatically isolates guided mode signal contributions and removes the effects of dispersive propagation, so as to allow source location with the clarity usually associated with bulk wave measurements. The principles of the measurement were discussed using the example of a source located some distance from the receiver. Ongoing work is examining the application of the principles discussed here to experimental data collected using the array transducer depicted in Figure (1). Results of these experiments will be incorporated into the QNDE presention. Future work plans to generalize the measurement for pulse-echo application, requiring mode isolation and dispersion compensation on both the transmit and reception leg of the pulse-echo measurement.

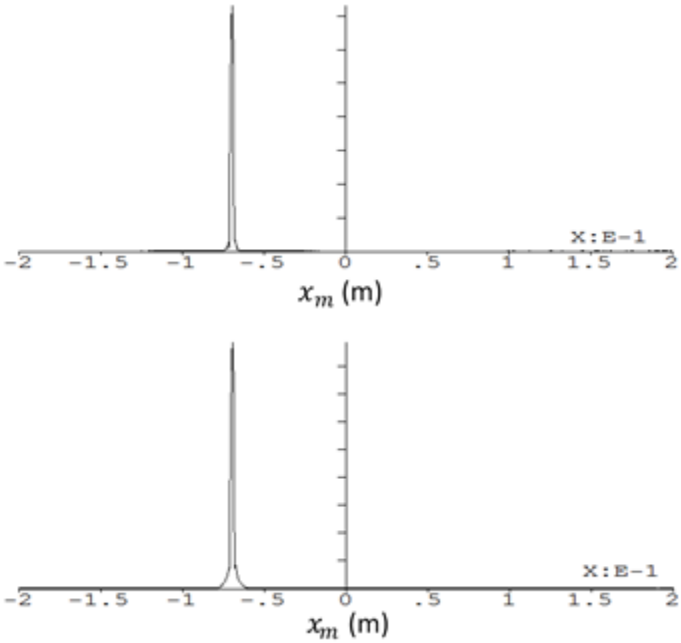

FIGURE 3: SOURCE LOCATION USING SYNTHETIC DATA: (TOP) A_0 MODE, (BOTTOM) S_0 MODE

ACKNOWLEDGEMENT

This work supported by the Industry/University Cooperative Research Center for NDE at Iowa State University

REFERENCES

[1] Wilcox, P. "A Rapid Signal Processing Technique to Remove the Effect of Dispersion from Guided Wave Signals," *IEEE Transactions on Ultrasonics, Ferroelectrics, and Frequency Control* Vol. 50 (2003): pp 419-427

[2] Roberts, R. Peters, E. and Chimenti, D. "Multimode Dispersion Compensated Pulse-echo Guided Wave Inspection." *AIP Conference Proceedings* Vol. 1650 No. 1 (2015): pp 622-630 https://doi.org/10.1063/1.4914662

[3] Auld, B. "General Electromechanical Reciprocity Relations Applied to the Calculation of Elastic Wave Scattering Coefficients." *Wave Motion* Vol. 1 (1979): pp 3-10